https://doi.org/10.5194/egusphere-2023-607
Preprint. Discussion started: 12 April 2023

COBALT DISTRIBUTION IN THE BOLEO STRATIFORM SEDIMENT-HOSTED ORE DEPOSIT; A TRANSTENSION RIFT BASIN IN CENTRAL BAJA CALIFORNIA PENINSULA, MEXICO.

Valente O. Salgado Muñoz1, Tina M. Niemi1 James B. Murowchick1, Alyssa Troia2, Anna Turi Maher3, Aldo Javier Jaime-Geraldo4,

[1]Faculty of Earth and Environmental Sciences, Division of the Natural and Built Environment, University of Missouri-Kansas City, Kansas City, MO 64110 U.S.A.

[2]Department of Geology, Cal Poly Humboldt, Arcata, CA 95521

[3]Department of Geography/Geology, University of Nebraska, Omaha, NE 68182

[4]Departmento de Geología, Universidad Autónoma de Baja California Sur. Mexico

Correspondence to: valentesalgadomunoz@mail.umkc.edu

Abstract.

The Miocene Santa Rosalia Basin, located in Baja California, Mexico, is a unique basin that contains the Boleo copper deposit. This basin provides a remarkable opportunity to study the early stages of tectonic evolution, volcanic activity, ore genesis, and sedimentary deposition in the incipient Gulf of California. Previous research suggested the presence of Co in areas between Cu and Zn, but the factors responsible for cobalt distribution in the basin remained unclear. This study utilized multiple methods, including historical geologic maps, core drilling, field measurements, XRF readings, petrographic analysis, and mineral composition analysis, to comprehend the Co mineralization of the Boleo Formation. Our research found Co anomalies in five localities, with the highest values situated at the base of a slump block in manto 3 near the Neptuno mine. The presence of elevated cobalt ~~readings~~, in areas with uplifted and eroded gypsum suggests the possibility of uplift and dissolution of earlier gypsum deposits, and an association with brine waters. Moreover, the result of the study indicates that gypsum interfingers with both the clastic facies and ore mineralization in mantos 1, 2, and 3, signifying a north-to-south expansion of the basin. The study also identified manganese oxides and Cu-Fe sulfides, including villamaninite, along laminated gypsum beds. The findings of this study suggest that cobalt enrichment is influenced by structural factors and occurs near subsurface evaporitic deposits. This supports the notion that cobalt mineralization forms near the redox front and through sulfate reduction processes. The study's findings offer valuable insights for further exploration and understanding of cobalt mineralization in similar geological settings.

https://doi.org/10.5194/egusphere-2023-607
Preprint. Discussion started: 12 April 2023

1. Introduction

Rift basins are elongated depressions as result of continental extension, lithosphere break up and are strongly influenced by its sedimentary filled. They are a crucial source of a wide range of ore systems from magmatic to hydrothermal due to its asthenosphere/mantle plume dynamics and thermal gradient. Stratiform sediment hosted copper deposits (SSHC) contain 20% of the copper and 80% of the cobalt world's resources, ~~they tend~~ to form in rift basins with unique conditions, involving a variety of processes including diagenesis, movement of brines across basins and the venting of hydrothermal fluids on to the seafloor or lakebed (Brown, 1992; Kirkham, 1989; Warren, 2000, 2016; Hitzman et al., 2017; Pirajno, 2018). The world's largest SSHC deposits are all situated in ancient basins and span an age range of Proterozoic to Paleozoic, presenting challenges in comprehending their evolutionary history (Hitzman et al., 2010, 2017). The Santa Rosalia Basin (SRB), located in the east-central peninsula of Baja California, Mexico, is a Miocene rift basin hosting the SSHC Boleo deposit (Fig. 1). The ~~sediments of the Santa Rosalia basin (~~SRB~~)~~ host the Boleo Formation, consisting of fluvial marine sedimentary rocks with nine stratiform mineralized beds called "mantos" (Fig. 2). The mantos consist of finely laminated claystone base (<2m), overlain by an intraclastic polymictic breccia of 20-2 m that thins to the east and capped by an Mn-oxide laminated claystone (<2m). Cu-Co mineralization appears along the claystone laminae, breccia matrix and fragments as finely disseminated grains (Conly et al., 2001). This basin offers a unique opportunity to analyze the formation mechanisms of copper and cobalt ores in a younger rift-related system. The present study focuses on the investigation of the distribution of cobalt within the basin. Previous studies have acknowledged that cobalt is concentrated in areas located between zones of copper and zinc enrichment (Conly et al., 2001) and is largely independent of the distributions of copper and zinc (Bailes et al., 2001). However, the exact distribution of cobalt remains unknown. This study aims to clarify this aspect.

In general, there is a significant limitation and understanding on the cobalt metal zonation, models of transportation, and depositional conditions of cobalt-rich mineralization within SSHC and the Boleo deposit is not the exception (Bailes et al., 2001; Conly, 2003; Muchez and Corbella, 2012). Because cobalt is found in the highest concentrations when integrated into other minerals, it is commonly extracted as a by-product. Cobalt is a transition metal with ionic radii of Co2+ and Co3+ very similar to the ionic radii of Mn4+, Fe2+, Fe3+, Ni2+, and Cu2+, thus in nature, shows a strong spatial association with Mn, Fe, Ni, and Cu (Smith, 2001; Hitzman et al., 2017). This unique geochemical property makes cobalt minerals transport and depositional conditions likely different than those controlling the distribution of copper minerals when present in the same ore deposit but remains poorly understood (Muchez and Corbella, 2012). In order to understand and identify the main entities responsible for the cobalt distribution within the Santa Rosalia Basin, we analyzed exploration drillhole assay data and portable XRF field measurements on main outcrops of the deposit. The current study seeks to create a spatial map of significant cobalt ore accumulation that can serve as a reference for future exploration programs targeting sediment-hosted copper-cobalt deposits.

https://doi.org/10.5194/egusphere-2023-607
Preprint. Discussion started: 12 April 2023

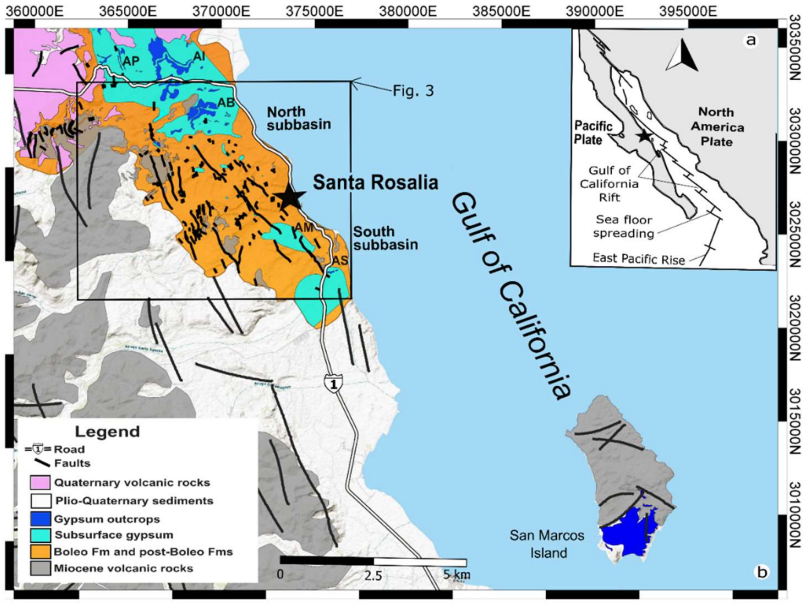

Figure 1 a) The Gulf of California lies along the transtensional plate boundary between the Pacific and North American plates. Seafloor spreading centers occur along short segments perpendicular to the trend of the gulf and are connected by right-lateral transform faults. b) Geologic map of the Santa Rosalia Basin and San Marcos Island region showing gypsum distribution in outcrop and subsurface. The star marks the location of the town of Santa Rosalia. Important drainages are marked as follows: AB=Arroyo Boleo, AI=Arroyo Infierno, AP=Arroyo las Palmas, AM=Arroyo Montado, AS=Arroyo Santa Agueda.

2. Geologic setting

The Gulf of California is a young oblique rift system that began 12-15 million years ago when subduction of the Farallon plate ceased beneath the North America plate and continental crust rupture began to form along rift and transtensional pull-apart basins (Lonsdale, 1989; Stock and Hodges, 1989; Fletcher et al., 2007; Umhoefer et al., 2018). Before the formation of the gulf, magmatic-arc volcanism prevailed in the region, depositing calc-alkaline andesitic lavas (24-13 Ma) followed by deposits of dacitic rocks indicating the final arc volcanism (13-11 Ma) known as the Comondú Formation (Hausback, 1984; Conly et al., 2005; Busby et al., 2020). The arc magmatism ceased around 12.5 Ma, and the rifting of the Gulf of California was initiated. Deposits of pyroclastic rocks (11- 8Ma), mark the transition from subduction to continental rifting in the Santa Rosalia basin (Conly et al., 2005; Busby et al., 2020). Two phases distinguish the formation of the gulf; a proto-gulf phase

https://doi.org/10.5194/egusphere-2023-607
Preprint. Discussion started: 12 April 2023

(11-6 Ma) evidenced by the extensional gulf province with early marine incursion in its southern mouth around 8 Ma (Umhoefer et al., 2018) and the modern gulf phase which developed with oceanic crustal formation in the offshore Guaymas Basin around 6 Ma (Miller and Lizarralde, 2013) and later in the southern gulf around 3.5 Ma (Sutherland et al., 2012). Busby et al. (2020) reported south of the Santa Rosalia basin, suites of post-subduction volcanic rocks known as "bajaites" (6.06 ± 0.27 Ma), comprised of high-magnesian andesite with 50%–58% SiO2 and MgO >4% and an adakite (>56% SiO2 and MgO <3%). These rocks associate spatially with a fossil slab imaged under central Baja (Calmus et al., 2003; Wang et al., 2013) and likely document post-subduction melting of the slab and subduction-modified mantle by asthenospheric upwelling related to rifting or slab breakoff (Busby et al., 2020). The age of the Boleo Fm has been constrained from ~7.1 Ma to 6.2 Ma Ma based on 40Ar–39Ar geochronology on a tuff marker bed known as Cinta Colorada and magnetostratigraphic correlation (Holt et al., 2000; Conly et al., 2005). However, new U-Pb dating of a zircon grain from the Cinta Colorada tuff yielding an age of 5.86 Ma ±0.12 Ma (Dorsey et al., 2022; Graettinger et al., 2022; Niemi et al., 2022) may redefine the age of the depositional period of the Boleo Formation to a younger age than previously assumed. Further constraints on the age of the Boleo Fm are based on the age determination of the volcanic rocks underlying the basin, which comprise calc-alkaline, rift transition, and post-subduction intrusive and extrusive volcanic sequences (Conly et al., 2005; Busby et al., 2020). The units of the Boleo Formation include a local basal conglomerate (<10 m), limestone (<5 m), thick gypsum (10-100 m), and four major clastic cycles that generally coarsen from claystone and siltstone at the base to sandstone and conglomerate at the top (Wilson and Rocha, 1955; Ochoa-Landín et al., 2000; Conly et al., 2005; Del Rio Salas et al., 2008). The mantos are found at the base of the clastic cycles and are labeled from the lower ore bed 4 to the upper ore bed 0 (Fig. 2), with subbeds 4a, 3a, 3aa, and one labeled "sin nombre" accounting for nine mineralized layers. The ore beds or mantos are not continuous across the Boleo Fm, and there is a division between the north subbasin that contains all the mantos, and the south subbasin that contains three manto units (2,1,0) (Conly et al., 2006; Salgado Muñoz, 2014; Ochoa-Landín, 1998). The north and south subbasin has been suggested to be separated by a topographic high of Comondú volcanic rocks (Ochoa-Landín, 1998.) (Figs. 1 and 2). Mantos are labeled in the drill logs from the top downwards as they are encountered, so there is uncertainty as to whether the mantos in the north subbasin correlate to the ore beds in the south subbasin. While there is uncertainty on the manto correlation, for this work, we will use the nomenclature used by the mining district for consistency and treat them as equivalent. Furthermore, the Boleo Formation is unconformably overlain by marine deposits that are constrained by microfossil biostratigraphy to between 5.57 and 4.6 Ma (Miranda-Martínez et al., 2017) and mark the transition to fully marine conditions in the basin (Fig. 2). This formation was originally named by Wilson and Rocha (1955) as the Gloria Formation but later renamed by Carreño (1981) as the Tirabuzón Formation. Finally, Plio-Quaternary Infierno and Santa Rosalia formations of marine origin are capped by Quaternary volcanic rocks and alluvium (Fig. 2).

https://doi.org/10.5194/egusphere-2023-607
Preprint. Discussion started: 12 April 2023

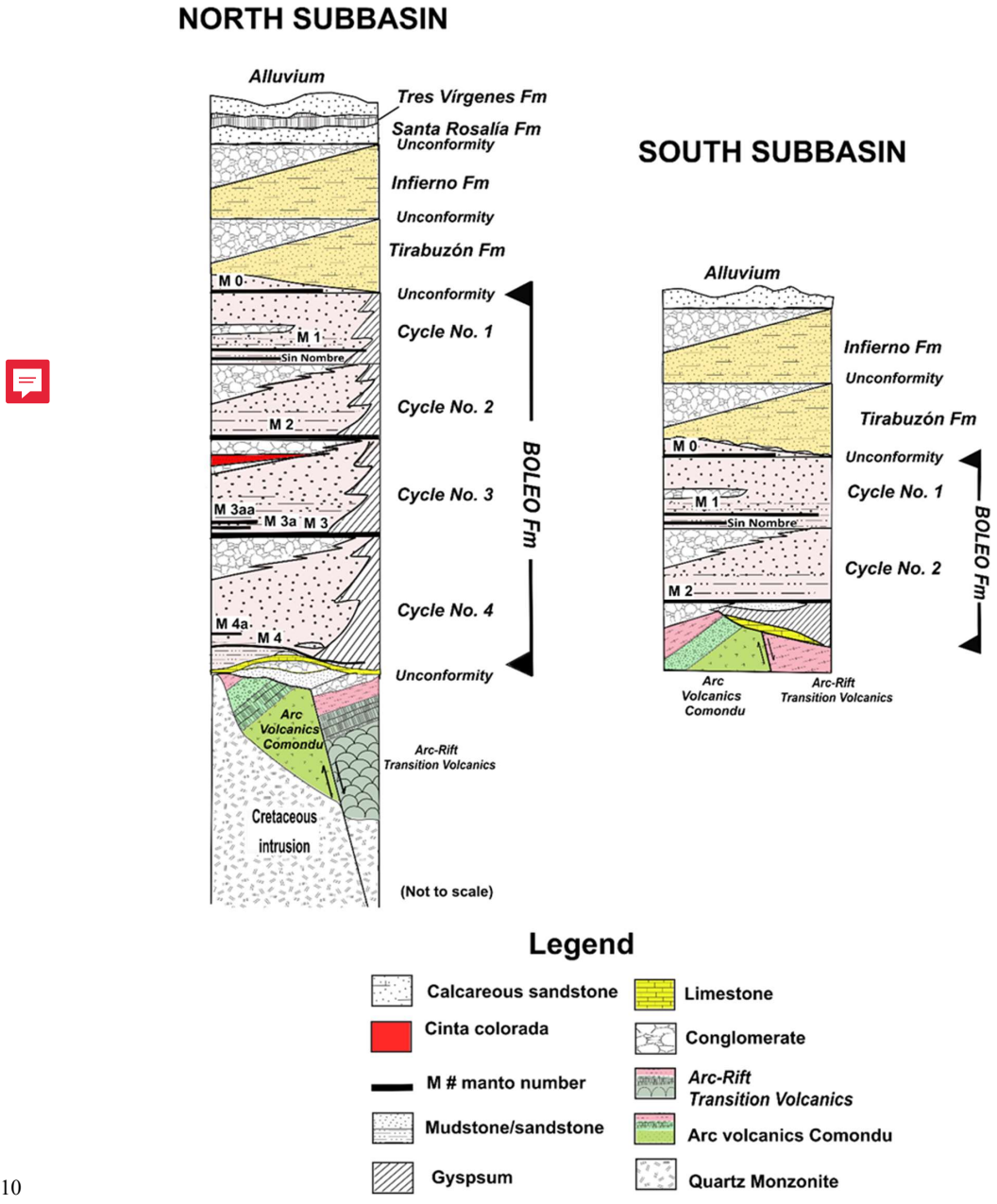

Figure 2 Schematic stratigraphic column of the north and south subbasin of the Santa Rosalia Basin based on interpretation of drillhole data and data presented in Wilson and Rocha (1955), Holt et al. (2000), Conly et al. (2006), Busby et al. (2020).

https://doi.org/10.5194/egusphere-2023-607
Preprint. Discussion started: 12 April 2023

3. Methods

3.1 Map and Drill hole Data

Two influential reports from the U.S. Geological Survey (U.S.G.S) by Wilson and Veytia (1949) on the Lucifer manganese deposit and Wilson and Rocha (1955) of the Boleo mining districts provide the most detailed lithologic descriptions and geologic maps of the Santa Rosalia region. The high-resolution geologic maps cover more than 168 km^2 at a scale of 1:15,000 and 1:10,000, respectively. The maps were based on the interpretation of aerial imagery, new topographic base maps, fieldwork, and a compilation of multiple maps dating from 1890 to 1948 provided by the mining company *Compagnie du Boleo* (Wilson and Rocha, 1955). In addition, Wilson and Rocha (1955) interpreted highly accurate maps of the mine workings and drill hole data contained in the company records. ~~This information was the basis for the eleven plates in Wilson and Rocha (1955) that include a topographic and geologic map, map of the location of subsurface mine workings and drill holes, structural cross sections, structural contour maps, columnar sections of shafts and drill holes, and maps of the distribution of gypsum and major faults.~~

Further exploration drilling since the 1950's provides plentiful new data on the Boleo deposit. From 1994 to 2004, Minera Curator, International Curator Resources Ltd subsidiary, conducted a diamond-bit core drilling campaign. From 2004 to 2011, Baja Mining Corp, through its wholly owned subsidiary Minera y Metalurgica de Boleo S.A. de C.V., also led another extensive drill program. This study utilizes these data, including depth to stratigraphic units, lithological descriptions, and elemental percent values determined by inductively coupled plasma–atomic emission spectroscopy (ME-ICP61) assay method (four acid "near-total" digestion to determine elemental ppm) from 1,419 drill holes from these explorations.

The comprehension of the tectonics, geology, and structural setting of the region and ore genesis concepts has increased substantially since the publication of Wilson and Rocha (1955) based on newly available information and new analytical methods. In this study, we compiled data from the 1950's U.S.G.S. reports, such as geologic maps, drill hole data and plates, with the most recent data from the latest exploration drilling campaigns. Geologic maps and plates with subsurface gypsum locations were digitalized in QGIS, and drill holes with lithological descriptions from Wilson and Rocha (1955) were added to the drill hole database of the recent drilling. Furthermore, the spatial locations of these drill holes were transformed from the local coordinates used by the former authors into the UTM coordinates. Leapfrog Geo software was then used to interpret in 3D the significant lithologic and elemental data (Fig. 3).

https://doi.org/10.5194/egusphere-2023-607
Preprint. Discussion started: 12 April 2023

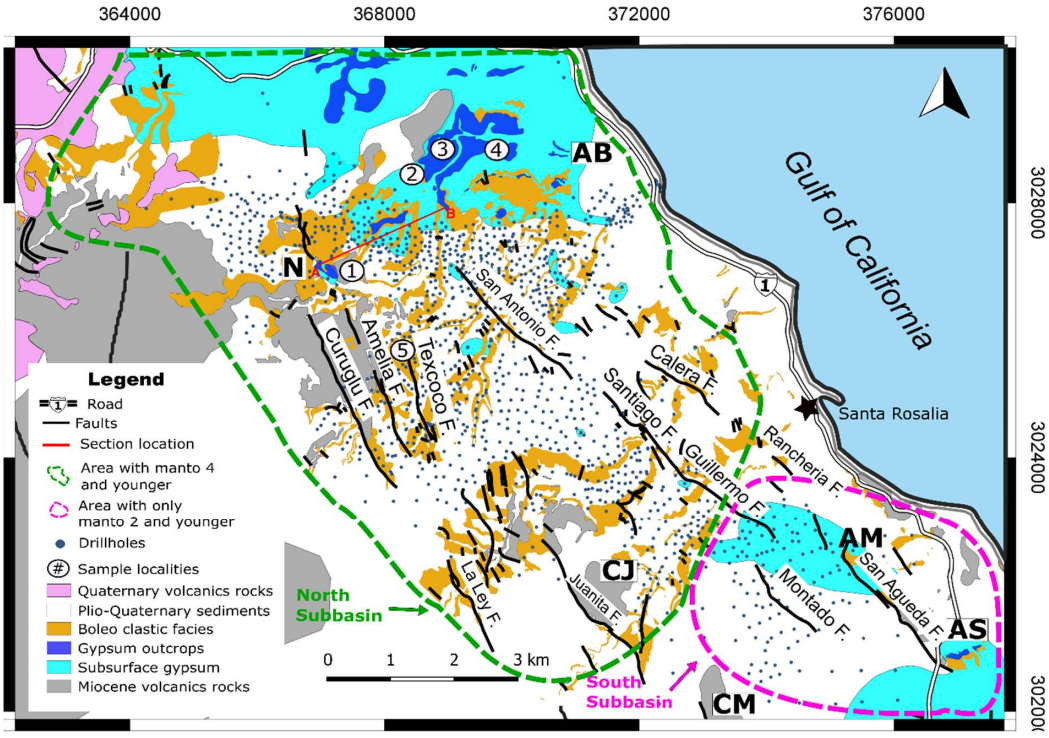

Figure 3 Map of a portion of the Santa Rosalia Basin (SRB) showing the location of the approximately 1500 drillholes analysed in this study. The outcrop pattern of the clastic and gypsum facies of the Boleo Formation and Miocene and Quaternary volcanic rocks is shown. The subsurface distribution of gypsum is based on recent borehole data and a plate map presented in Wilson and Rocha (1955). Gypsum outcrops and sample localities are shown with numbers at the Neptune (N) mine and Arroyo Boleo (AB) sites. Isolated hills of late Miocene basaltic andesite, Cerro Juanita (CJ) and Cerro Montado (CM). Names for prominent faults in the SRB after Wilson and Rocha (1955).

3.2 Field Data

We used a portable Thermo Scientific Niton XL2 tube-based x-ray fluorescence (XRF) analyzer to locate cobalt enrichment within the outcrops of nine locations of the Boleo Formation that showed higher concentration in the exploration drilling data. These outcrops were in the vicinity of the Arroyo Boleo, Neptuno and Texcoco areas (Fig 3). Because Fe and Ni have spectral peaks similar to cobalt's primary and secondary peak in energy dispersive XRF, hand samples with high

https://doi.org/10.5194/egusphere-2023-607
Preprint. Discussion started: 12 April 2023

anomaly cobalt were collected. 25 hand samples from the 150 portable XRF readings of the main outcrops were collected and analyzed for composition by X-ray spectroscopy and powder X-ray diffraction (XRD).

We also conducted detailed stratigraphic measurements of the main outcrops in Arroyo Boleo, Neptuno and Texcoco area. Samples from the clastic sequence and laminated gypsum beds were collected for petrographic analyses. Powder X ray diffraction were analyzed by using a Rigaku Miniflex automated diffractometer, with Cu and Co cathode operating at 35kV, 15mA, 5-60° 2θ in step scan mode at 0.05°/step with 3 seconds count time/step. Thin sections from the clastic sediments and laminated gypsum were analyzed for minor metal phases using semiquantitative scanning electron microscopy-energy dispersive X-ray spectroscopy (SEM-EDS). The SEM-EDS analysis was conducted using a Tescan Vega 3 L.M.U. equipped with a Bruker Quantax energy dispersive spectroscopy system at the laboratories of the University of Missouri-Kansas City.

4. Results

4.1 Cobalt Metal Distribution in the Santa Rosalia Basin

The Boleo ore deposit extends for more approximately 90 km^2 and has delineated reserves of 70 dry Mt grading 1.29 % Cu, 0.089 % Co, and 0.62 % Zn (Bailes et al., 2001). Most of the copper-cobalt mineralization in the Boleo deposit varies among sulfide-oxide facies and occurs as disseminated grains in claystone, within breccia matrix and intraclasts, as well as open-space infillings (Wilson and Rocha, 1955; Ochoa-Landín, 1998; Conly et al., 2001). The mantos are either in contact with conglomerate facies or on a basal claystone above the conglomerate which is not always mineralized (Fig. 2). Average cobalt ore grade for stratiform sediment hosted copper deposits worldwide is about 0.3% but with ore grade ranges from 0.026% to 1.08% (Horn et al., 2021). In Fig. 4a, we used drill hole assay data with values above 0.1~~00~~ % cobalt grade to show the distribution of cobalt mineralization of economic importance within the SRB. From these data, four main centers of concentration are recognized with high Co values, three in the north subbasin and one in the south subbasin.

Cobalt mineralization in the north subbasin is predominantly present within the Arroyo Boleo, Neptuno and Texcoco area. Cobalt grade above 0.150 % is primarily in manto 3 and manto 3a. The cobalt mineralization within the Neptuno area is around and below olitostromes. We found a black manganese-cobalt rich layer below one of the olitoliths in the Neptuno area (Fig. 5a and 5b). The other two centers in the north subbasin of cobalt grade value are in Arroyo Boleo in proximity to the main gypsum exposures looked in this study. The fourth concentration of cobalt values greater than 0.150 % is within the south subbasin and is concentrated in manto 1. The cobalt values lie between two main NW-trending faults of the Boleo district—the Montado and Santa Agueda faults. In contrast with cobalt distribution, copper mineralization concentrations lie mainly in the north subbasin in manto 3 and the south subbasin in manto 1. The distribution of copper mineralization in the north subbasin is primarily in the central part of the Boleo deposit and displays a N.W. trend (Fig. 4b).

https://doi.org/10.5194/egusphere-2023-607
Preprint. Discussion started: 12 April 2023

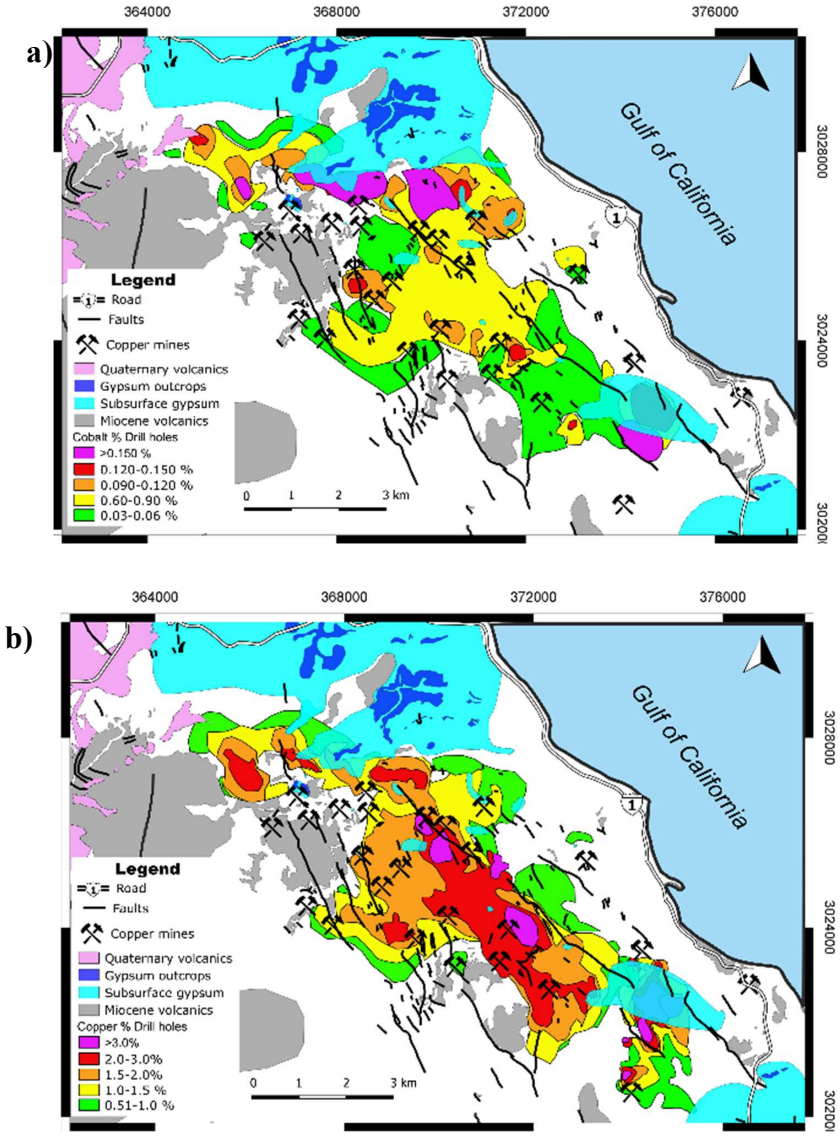

Figure 4 Copper-cobalt distribution near evaporites deposit of the Boleo ore deposit. a) Cobalt grade mineralization considering all mantos in the north and south subbasin of the Boleo deposit showing strong affinity to the presence of nearby evaporites edging the basin and main faults. b) Copper grade distribution in the Boleo deposit in all mantos shows a different spatial distribution closer to the center of the basin and linked to the major faulting of the basin.

https://doi.org/10.5194/egusphere-2023-607
Preprint. Discussion started: 12 April 2023

Similar Cu/Zn ratios for mantos 1 (7.07%) and 3 (7.23%) are consistent with the findings of Conly et al. (2006). However, the Co/Zn ratio for manto 1 (0.36%) is different from manto 3 (0.726%) described by the previous author. In addition, manto 2 was found to have a higher Cu/Co than other mantos with 2.23%. Figure 6 shows the distribution of cobalt for values above 0.10~~0~~ percent in different mantos. Cobalt enrichment is present within all the mantos except mantos 4 and 4a. Manto 3 has the highest-grade concentration, followed by manto 3a. Manto 3a immediately overlies manto 3, but its stratigraphic proximity is often complicated to distinguish between them (Bailes et al., 2001; Conly, 2003). Manto 3aa overlies 3a and is mainly constrained to the areas surrounding the San Antonio fault and the gypsum of Arroyo Boleo in the north subbasin. Manto 3 is not present within the south subbasin (Fig. 7). Manto 2 is distributed within both the north and south subbasins, but higher cobalt values are found within the south subbasin (Fig. 7). In addition, cobalt values in manto 1 are only present in the south subbasin. Moreover, when elevation is plotted against the easting direction (Fig. 7), we can observe how the north subbasin cobalt enrichment in manto 3 switches into a manto 2 with a similar elevation as manto 3 get closer to the edge of the north and south subbasin. Furthermore, the high cobalt grade moves southeast, and the high-grade cobalt values of manto 1 are higher than other mantos but with few significant cobalt values in manto 2.

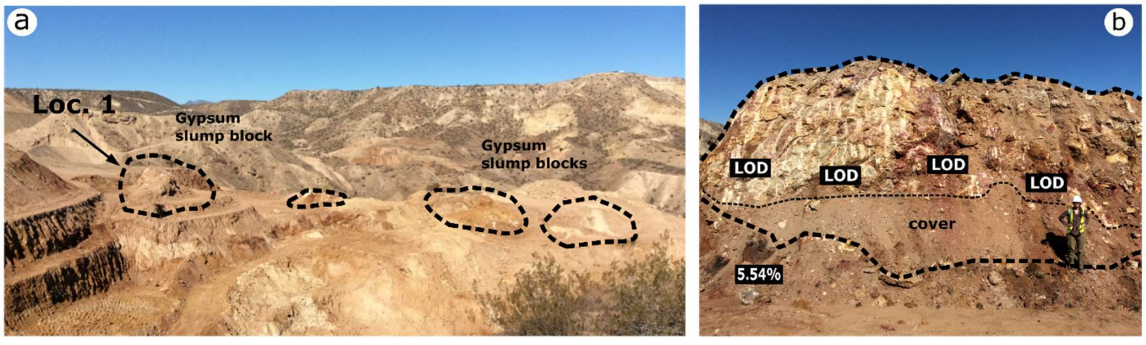

Figure 5 Open pit mining near the historic Neptuno mine (Fig. 3) exposed large gypsum slump blocks (dashed lines) that were stratigraphically within the manto 3 layer at our locality 1 study site. a) Overview photograph of the Minera Boleo surface mine from 2019 showing large olistoliths of gypsum left *in situ* when the ore deposit was mined. View toward the west (260°). Surface mine bench height is approximately 10 m. b) A large gypsum slump block shown in figure 5a locality 1 presenting XRF readings within and below gypsum slump block. Within the gypsum most readings for cobalt are below the limit of detection (LOD). A concentration of 5.54% weight percentage cobalt is found in manto 3 below one of the slump blocks of gypsum.

https://doi.org/10.5194/egusphere-2023-607
Preprint. Discussion started: 12 April 2023

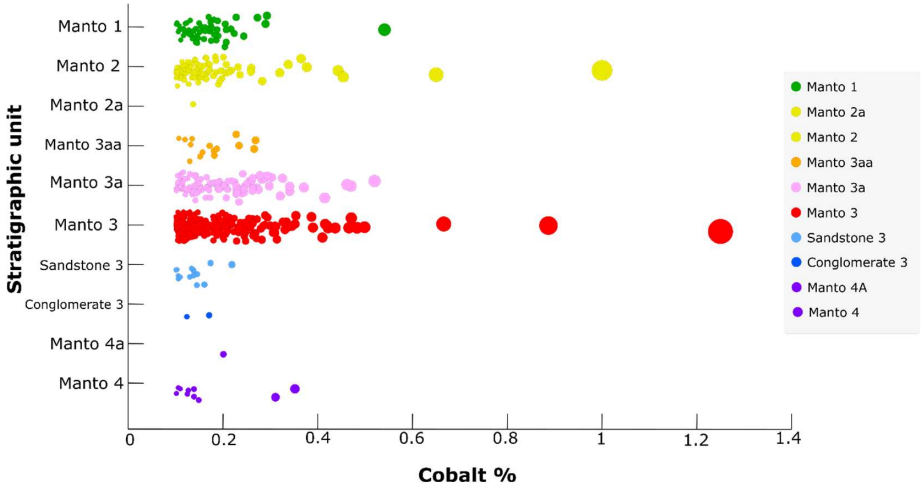

Figure 6 Distribution of cobalt values above 0.100% for each manto of the Boleo deposit. Manto 3 presents main cobalt enrichment, followed by manto 3a and manto 2 in the north subbasin. Manto 1 cobalt enrichment is only present in the south subbasin.

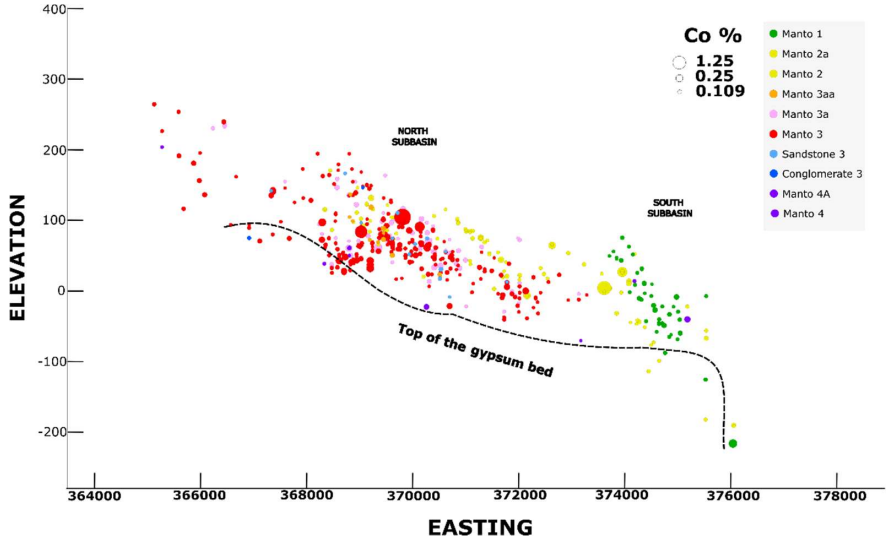

Figure 7 Graph of all cobalt values above 0.1% plotted by manto number and elevation from drillhole logs along a NW-SE cross section. The dash line marks the top elevation of the subsurface gypsum. The color of the data points represents the manto number as recorded in the drill logs with manto 1 at the top and manto 4 at the bottom. More significant data point are greater cobalt values.

https://doi.org/10.5194/egusphere-2023-607
Preprint. Discussion started: 12 April 2023

High cobalt values seem to correlate with subsurface gypsum bodies and major faults in the district. Five main faults San Antonio, Guillermo, Santiago, Montado, and Santa Agueda faults (Fig. 3), all with a similar strike of 315° and dip amounts of 70-78° in the SW direction and considerable displacement from 15 to 250 m, are adjacent to high cobalt concentrations. The strike and dip of the main faults in the north and south subbasins are consistent with the kinematic analyses performed by Angelier et al. (1981) that describe west-dipping normal faults with a dextral, strike-slip component in the SRB.

4.2 Cobalt Concentrations Near Evaporitic setting

Gypsum of the Boleo Formation was deposited extensively throughout the Santa Rosalia basin. The primary exposures are located within Arroyo Boleo, northwestward in Arroyo de las Palmas, and in Arroyo del Infierno where a gypsum mine is located (Figs. 1 and 3). In the southern portion of the SRB, key exposures are in Arroyo Montado and Arroyo Santa Agueda, but they extend as far south as San Marcos Island (Fig. 1). Data from drill holes provide the location of the subsurface distribution of gypsum and help to define two depocenters for evaporite accumulation in the north and south parts of the SRB with isolated and scattered subsurface between the two areas (Fig 1). ~~Bolco~~ gypsum outcrops are more prevalent in the north than in the south. The gypsum member is more extensive and has several meters in thickness (10-120m) than the south, where there are smaller outcrops and fewer meters in thickness (10-15m) Gypsum outcrops lie near the coast and are mainly east of the areas comprising the Cu-Co-rich ore deposits and extend northwest and southeast of the ~~Bolco~~ mining district (Fig. 3). Copper mineralization is concentrated in a north and south subbasin within the SRB (Fig 3). The north subbasin is defined by the limit of mantos 3 and 4, and the south subbasin is defined by areas with only manto 2, 1 and 0. Four major coarsening-upward clastic cycles that grade from claystone and siltstone at the base to sandstone and conglomerate at the top that contain nine mantos (ore beds) from manto 0 to 4 are found in the north subbasin (Figs. 2 and 3). However, the south subbasin only contains the upper two clastic cycles and four mantos from 0 to 2. Contrary to previous publications that place the gypsum in a basal position in the Boleo Fm (Wilson and Rocha, 1955; Ochoa-Landín et al., 2000; Bailes et al., 2001; Conly et al., 2005, 2006; Del Rio Salas et al., 2008; Conly et al., 2011; Del Rio-Salas et al., 2013), analyses of drill hole data indicate that gypsum interfingers with both Boleo clastic facies and ore mineralization at mantos 4, 3, 2, 1. Gypsum drill holes intersect in the northwest portion of the north subbasin (Neptune mine area) and are found both above and/or below manto 4 (Fig. 3). In the north and southwest of the north subbasin, gypsum intersects lie beneath manto 3 and interfingers with clastic layers below the ore bed. Below manto 2, gypsum intervals are present in the exploration drill holes with a wide distribution across both subbasins and the central part of the basin (Fig. 3). Moreover, southwest of the Santa Rosalia town, Wilson and Rocha (1955) described 14 m of gypsum below manto 2 encountered in one of the underground workings. Further southeast, in Arroyo Montado and Arroyo Santa Agueda, the gypsum bed reaches 40 m in outcrop and ranges from 14 to 70 m in the subsurface.

https://doi.org/10.5194/egusphere-2023-607
Preprint. Discussion started: 12 April 2023

In this study, 150 XRF readings from clastic and gypsum outcrops resulted in 23 significant cobalt anomalies with values above 0.050 Co % (Table 1) from five localities (Fig. 3). Locality 1 is in a Minera Boleo mining company open pit mine adjacent to the westernmost outcrop of gypsum near the old Mina Neptuno mine. Localities 2 to 4 are gypsum exposures located in the incised canyon and mouth of Arroyo Boleo. Lastly, locality 5 is located near the area of Texococo mine west of arroyo Boleo.

At the locality 1 ~~Neptuno site~~, an isolated outcrop of gypsum (300 m by 150 m) overlies Upper Miocene basal limestone and the volcanic rocks as mapped by Wilson and Rocha (1955) (Fig. 8). In 2019, during open-pit mining of manto 3 east of the old Mina Neptuno area (Fig. 3) Minera Boleo company encountered large detached and isolated gypsum blocks (Fig. 5 and Fig. 8). The gypsum at this location was heavily altered and red in color. Primary evaporitic textures were not visible. Multicolored impregnations indicated the presence of limonite, hematite, and manganese oxides. The gypsum blocks are approximately 10 m by 6 m or larger and are embedded within the clastic cycle that contains manto 3 mineralization. Gypsum slump blocks or olistoliths in the Minera Boleo open pit mine show that the early basinal sedimentary fill extended farther to the west-southwest and was uplifted during syndepositional faulting of the Boleo Formation. These data suggest that the early basinal faults became inactive, and the footwall uplifted as the depocenter migrated basinwards. Large areas of evaporites along the margins of the northern subbasin have likely been similarly eroded or entirely removed by dissolution. The highest cobalt value found in our fieldwork is at locality 1 near Neptuno mine at the base of a slump block where a black silty sand, moderately sorted, very poorly consolidated sediment showed values of 49.96 % Mn, 1.33% Cu and 5.59% Co on our XRF.

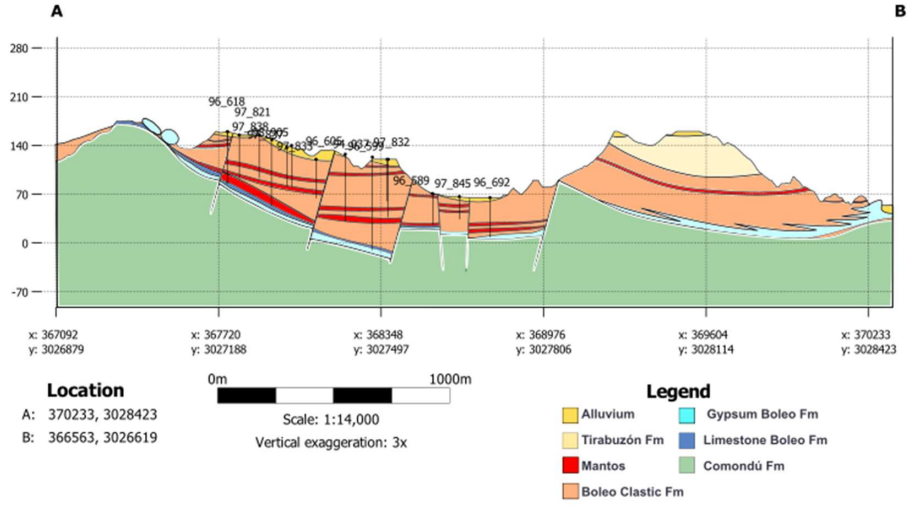

Figure 8 Section A-B from the Boleo Formation looking northwest illustrating olistoliths in Neptuno area (location shown on Fig. 3)

https://doi.org/10.5194/egusphere-2023-607
Preprint. Discussion started: 12 April 2023

A 40-m-high outcrop of gypsum is exposed in an incised canyon of the lower reaches of the Arroyo Boleo at Localities 2 and 3 (Fig. 3). At these locations, anticlinal folding allowed us to measure a >100 m stratigraphic section of gypsum and interbedded clastic layers (Fig. 9a). The base of the section is a 35-m-thick lower gypsum bed that is separated from the upper laminated gypsum bed by an interbedded 6- to 15-m-thick clastic layer. Both gypsum beds exhibit primary and modified primary depositional textures that reveal diverse evaporitic sedimentary facies ranging from finely laminated, layers of upright selenite crystals, layers with laminates alternating with upright crystals, gypsrudites with blocks of redeposited gypsum clasts, and other sabkha and subaerial facies (Schreiber et al., 1976; Hardie et al., 1985; Matano, 2007; Schreiber et al., 2007; Kendall, 2010; Warren, 2016; Salgado Muñoz et al., 2018). Locality 2 is at the boundary between the clastic bed and the upper gypsum bed (Fig. 9b). At this contact, the uppermost layer of the clastic bed consists of a 0.50-m-thick red sandy conglomerate and thin, very fine sandstone crosscut by abundant satinspar veinlets. This layer is overlain by a 0.5-m-thick, weakly mineralized, white-altered gypsum layer with wavy laminations of iron oxide-stained clay and silt. XRF readings from the white altered gypsum revealed 6.18% Fe, 1.27 % Mn, 0.493% Cu, and 0.341 % Co values. At the base of the upper gypsum bed above this layer is a 1.8-m-thick massive gypsum bed with randomly oriented clusters of selenite crystals denoting a return to subaqueous evaporite deposition.

The sample site at locality 3 is within a laminated gypsum sequence with white, brown, green, black layers and visible impregnations of limonite, manganese oxides and copper oxides mineral (Fig. 9c). XRF measurements of the gypsum at this site yielded cobalt values as high as 0.914% (Fig. 9c). Within the laminated sequence, evidence of synsedimentary deformation and seismites are common indicating active tectonism during deposition. Two hand samples were collected for XRD and SEM/EDS analysis. XRD analysis of sample 16-1B of the laminated sequence ~~only~~ revealed gypsum as the main mineral. The SEM analysis showed a trace mineralogy that includes sphalerite, celestite, and villamaninite concentrated along bedding planes (Fig. 10a). A sample taken next to the location of 16-1B, sample 16-3 with green copper stains and high cobalt values, revealed bedded Cu, Co, Fe, and Ni rich minerals, villamaninite, celestite, Cu-Co oxides, with a gypsum crystal growth displacing Cu-Co-Fe-Ni crystals laminations along a bedding plane under the SEM/EDS analysis (Fig. 10b).

https://doi.org/10.5194/egusphere-2023-607
Preprint. Discussion started: 12 April 2023

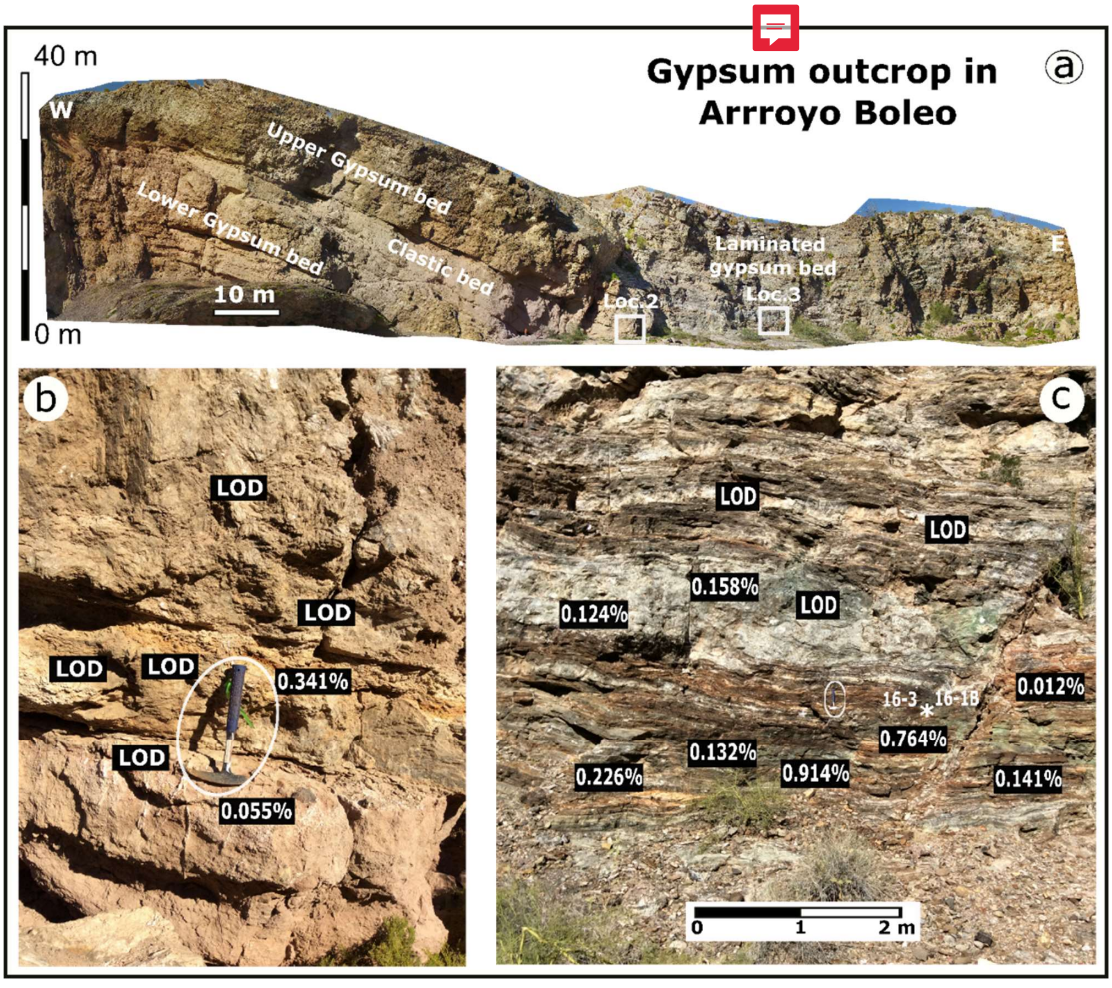

Figure 9 a) Orthophoto mosaic showing the outcrop of the lower gypsum bed, interbedded clastic bed, and the upper gypsum bed along the north side of the lower Arroyo Boleo drainage. Localities 2 and 3 are marked with a box. b) Photograph of the contact between the uppermost clastic bed and the upper gypsum at locality 2 showing XRF measurements of cobalt. Oval around a 35-cm-long rock hammer for scale. c) Photograph of the laminated gypsum at locality 3 showing the sites with >0.1 % cobalt concentrations based on XRF measurements. The location of samples 16-1b and 16-3 is marked with an asterisk. LOD=limit of detection for cobalt levels.

https://doi.org/10.5194/egusphere-2023-607
Preprint. Discussion started: 12 April 2023

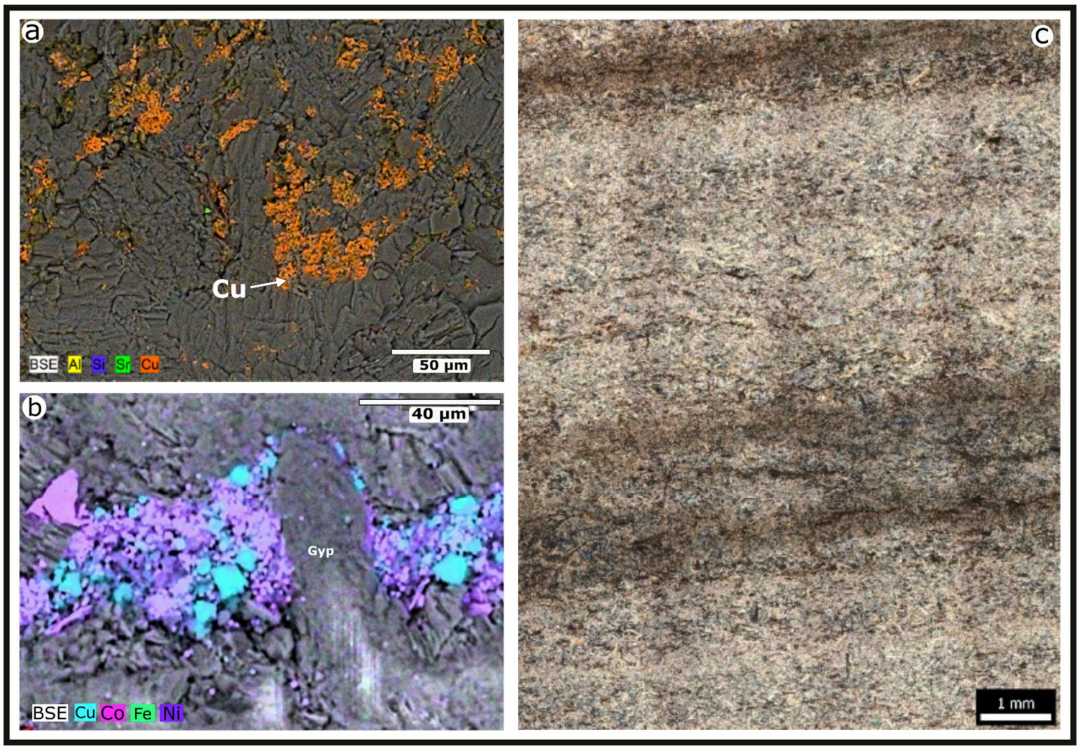

305 **Figure 10** An SEM/EDS image a) laminated gypsum sample 16-1B showing celestite $SrSO_4$ and Covellite (CuS) concentrated along laminae. b) Elemental map of sample 16-3 showing laminae of Cu, Co, Fe, and Ni-rich minerals. A gypsum crystal displaces the mineralized layer. c) Thin section showing gypsum bands with thin brown micrite laminae.

Locality 4 is the easternmost sample site within the laminated gypsum sequence, where one XRF reading showed
310 values of 2.85 % Fe, 0.121 % Mn, 0.77 % Cu and 0.116 % Co. This outcrop is near the mouth of Arroyo Boleo at the old quarry known as Yeso mine, where the former *Compagnie du Boleo* mined gypsum for its smelter (Wilson & Rocha, 1955). The gypsum at this locality is a laminated gypsum with orange to grayish black color, as the gypsum of location 3.
Locality 5 is from the upper clastic sequence of the Boleo Formation, near the Texcoco mine area. In this locality we were able to access manto 1, 2, 3a and 3 for XRF analysis (Table 1).
315

https://doi.org/10.5194/egusphere-2023-607
Preprint. Discussion started: 12 April 2023

Location	Reading #	Co	Cu	Zn	Mn	Fe
Loc 1	7	5.54	1.335	1.616	49.969	39.096
Loc 2	37	0.341	0.493	0.498	1.274	6.184
Loc 3	29	0.124	0.445	0.021	0.52	0.392
	36	0.158	0.358	0.038	0.457	2.08
	41	0.914	3.17	<LOD	1.94	0.481
	42	0.132	1.691	0.022	0.185	1.483
	44	0.764	3.905	<LOD	3.763	1.503
	57	0.141	5.468	<LOD	0.068	1.032
Loc 4	35	0.086	LOD	0.025	0.156	4.959
	34	0.116	0.077	0.025	0.121	2.858
Loc 5						
manto 1	2	0.071	0.073	0.104	17.005	3.178
	4	0.118	0.04	0.172	19.58	2.895
	5	0.642	0.237	0.551	93.954	2.074
manto 2	13	1.703	0.14	5.103	78.913	12.549
	14	2.075	0.307	5.984	73.399	17.558
	16	1.126	8.459	2.63	79.751	6.011
	17	2.36	7.808	4.387	66.763	14.968
manto 3a	8	4.557	1.057	1.994	68.109	24.138
	9	4.051	5.681	3.475	63.303	18.516
manto 3	13	0.049	1.127	0.451	0.238	4.94
	14	0.152	3.411	0.608	12.234	3.202
	19	0.514	13.987	2.129	0.26	82.67
	21	2.46	14.398	1.581	66.551	10.431

Table 1 Significant cobalt values along with copper, zinc, manganese, and iron values in weight percentage as determined by handheld XRF methods from gypsum and mantos outcrops exposed in an open pit mine near Mina Neptuno (locality 1) and Arroyo Boleo (Loc. 4-5).

Vertical stratigraphic distribution of cobalt within the mantos is illustrated in (Fig. 11). Most of the minerals identified by x-ray diffraction show the presence of covellite, nontronite, hematite and anorthite minerals (Fig. 12). The thickness of manto 1 is about approximately 1.75 m and exhibits a lenticular interbedded sand silty mud with Mn rich lenses coarsening upwards (Fig. 11a-~~11~~b). Manto 2 is about 2.25 m thick, and the base is composed of 40 cm of wavy laminated to planar bedding silty clay, with scattered manganese oxides lenses along laminae. It grades into a parallel interbedded sand and mud bed of 2 cm to 3 cm thick and is crosscut by manganese oxides veinlets of 2 to 3 mm wide. The silt and clay beds are overlain by a 15 cm sinter-like nodular lenses, at the lower contact of the silica rich sinter-like structure, thin 1.5 mm green copper oxides laminations were observed. Above the nodular sinter lenses, a 1.72 m thick extremely weathered

https://doi.org/10.5194/egusphere-2023-607
Preprint. Discussion started: 12 April 2023

stockwork breccia with gypsum and black Cu-Co-Mn oxide veinlets is present, this unit shows a gradational contact with a medium grain sand and silt bed rocks (Fig. 11c-~~11~~d). Moreover, the base of manto 3a in the Texcoco area is composed of a 25 cm thick green and brown silty clay laminae beds of 1 mm thickness. Overlain this green and brown laminated bed, 70 cm thick weathered white to yellowish interbedded mud and silt bed with < 1.0 mm thick wavy discontinuous nonparallel Cu-Co-Mn veinlets is present. This interbedded mud and silt are capped by a 25 to 10 cm thick wavy curved Cinta Colorada (Fig. 11e-~~11~~f). Manto 3 does not outcrop; however, it can be accessed through the abandoned Texcoco mine. Manto 3 has a thickness of 2.7 m, and the base is composed of interbedded siltstone and laminated clay, whiteish and yellow color, overlying a volcanoclastic conglomerate. Above the siltstone clay interbeds, lies a 1.5 m copper-rich convolute laminated claystone with hematite mineralization spots in the upper contact. Immediately above, a polymictic breccia with rip-up intraclast and manganese nodule in the upper section.

https://doi.org/10.5194/egusphere-2023-607
Preprint. Discussion started: 12 April 2023

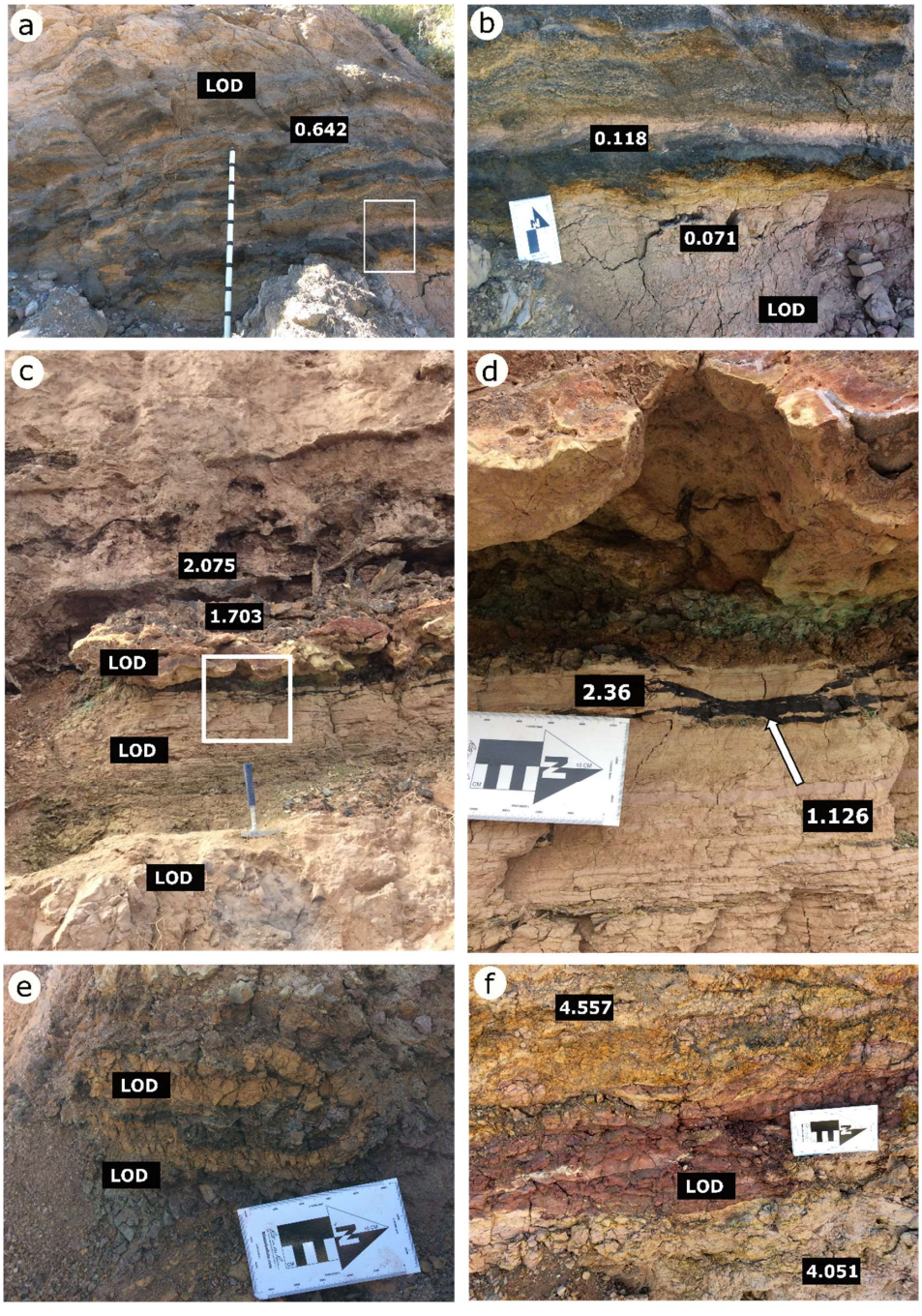

https://doi.org/10.5194/egusphere-2023-607
Preprint. Discussion started: 12 April 2023

Figure 11 a) illustrates Manto 1, with a thickness of 1.75m and consisting of lenticular beds of interbedded sand and silty mud, marked by Mn-rich lenses rich in Co. b) provides a closer look at the lenticular shape of the Mn-rich lenses. c) depicts Manto 2, which is approximately 2.25 m thick and has a base of 40cm of silty clay with scattered manganese oxide lenses. This clay grades into a 2-3 cm thick interbedded sand and mud bed intersected by manganese oxide veinlets rich in Co. A 15 cm sinter-like nodular lenses is located above the clay beds, with a 1.72m weathered stockwork breccia filled with gypsum and black Cu-Co-Mn oxide veinlets above the nodules. d) shows a closer look at the interbedded sand and mud beds and the manganese veinlets. e) and f) depict Manto 3a in the Texcoco area, consisting of a 25cm green and brown silty clay bed overlain by a 70 cm weathered interbedded mud and silt bed with wavy Cu-Co-Mn veinlets, capped by a 25-10cm thick Cinta Colorada.

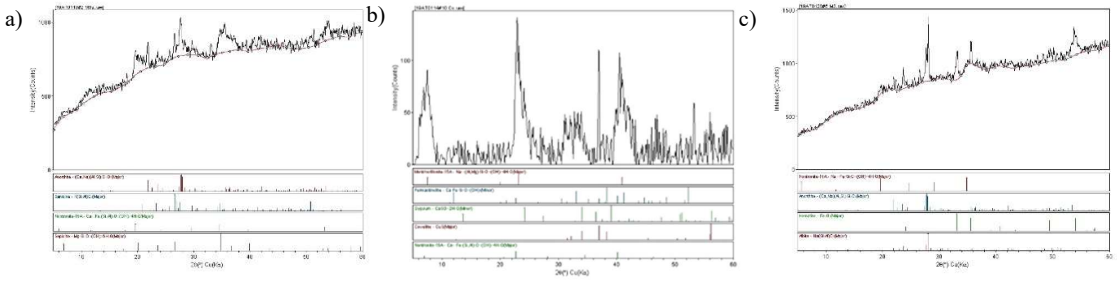

Figure 12 a) X-ray diffraction of manto 2 with presence of covellite, ferro actinolite, nontronite and gypsum. b) Manto 3a x-ray diffraction analysis shows presence of anorthite, sepiolite, sanidine and nontronite minerals. c) Manto 3 shows presence of albite, hematite and anorthite minerals in this study.

5. Discussion

This study maps the cobalt distribution within the Boleo deposit and expands in the gypsum distribution within the Santa Rosalia basin in the surface and subsurface. It enhaces on the plate map of Wilson and Rocha (1955) with a better understanding of how the clastic sediments that contain the Cu-Co ore deposits interfinger at the margins of coeval evaporitic deposition. Cobalt values above 0.120 % are positioned within the presence of gypsum or within a halo of ~700 m of former gypsum deposits and fault structure, similar to ore type reported distances of other Cu-Co sediment-hosted provinces (Selley et al., 2018). Moreover, copper-cobalt ore layers called mantos developed at the base of four major coarsening upwards clastic cycles driven by tectonic subsidence along faults active during deposition due to the incipient rifting of the Gulf of California. Clastic layers within the gypsum exposed in Arroyo Boleo indicate that the area of the evaporite deposition shrank as clastic sediment poured into the basin. Overlying laminated gypsum suggests that basin water deepened as the evaporite basin expanded, similar to the fluvial-delta cycles in the Boleo ore deposits. Drill hole data from

https://doi.org/10.5194/egusphere-2023-607
Preprint. Discussion started: 12 April 2023

Wilson and Rocha (1955) indicate that the Boleo deposits were known to have 4 major mantos cycles north of Santa Rosalia and only two major mantos in the south. Based on limited drill hole data, Ochoa-Landín et al. (2000) divided the Santa Rosalia basin into two subbasins and suggested a N-S striking ridge of Comondú volcanic rocks separating the north and south subbasins. Our analysis of drill hole data did not find a volcanic ridge but found scattered gypsum bodies along with the trend of these two depocenters.

Furthermore, stratigraphic data from drill logs suggest an interfingering of gypsum with mantos 2 and 3. These data indicate that the basin expanded from the north to the south subbasin. The gypsum in the SRB was deposited in an evaporitic basin fed by marine waters based on $^{87}Sr/^{86}Sr$ ratios of the gypsum (Ortlieb and Colleta, 1984; Conly et al., 2006). Gypsum within the Boleo Fm indicates that marine waters were once connected either by overflow or seepage to the evaporitic basin at the time of deposition, and saline groundwater likely underlaid the basin. In the Neptune area of the western part of the SRB where gypsum is uplifted and eroded, our high cobalt XRF measurements show that fluids within the slump blocks were enriched in cobalt. The slump block of gypsum within manto 3 alludes to a possible uplift and dissolution of earlier gypsum deposits at the time of deposition of the mantos and association with a marine aquifer likely playing a pivotal role in the salinity of groundwater and fluids during Boleo ore deposition.

High $^{87}Sr/^{86}Sr$ signatures of gypsum present on the mantos as well as low values of the δ18O, and δ34S in manto 3 barites from marine sulfate trapped within the pore's sediments, suggests presence of an evaporitic setting during deposition of the mineralization (Bailes et al., 2001; Conly, 2003; Conly et al., 2006, 2011; Del Rio-Salas, 2011). Conly et al. (2006) reported low strontium values on a gypsum mound sample from the Neptune area, he attributed the low strontium values to a strong influence of fresh water and the interaction of the seawater to the underlying volcanic rock sequence. Seawater basin modification and seawater interaction with volcanic rocks can lead to less radiogenic strontium isotopes than normal seawater on the gypsum, but low Sr isotopic composition can also form in bottom waters of dissolved older evaporites, as well as alteration during burial diagenesis by interstitial water with different composition from the contemporaneous seawater (Müller et al., 1990). Furthermore, exposures in the Neptuno surface mine show that at the time of manto 3, blocks of gypsum had been uplifted and recycled into a newer sedimentary basin. This inversion from evaporite deposition to erosion is typical of the early evolution phases of rifting as early faults become inactive and the basin depocenter migrates basinward (Gawthorpe and Leeder, 2000). Cobaltiferous smithsonite, spherocobaltite, a hydrous cobalt $CaCO_3$, carrollite, linnaeite and cobalt bearing sulfides as intergrowth within chalcocite as well as chalcopyrite cobalt-rich rims have been reported in the Boleo ore (Wilson and Rocha, 1955; Bailes et al., 2001; Conly, 2003). Carrollite and linnaeite are assumed to be at trace level; thus, neither cobalt sulfide mineral can account for the total Co grade (Conly, 2003). According to Conly et al. (2011), manganese oxides contain at least 10 percent of the Cu and Co content of the mineralized beds or "manto" is consistent in locality 1, where an XRF reading yielded 49.96 % Mn and 5.54% Co and 1.33% Cu was found. In this study, we identified Mn and Cu-Co oxides, including a Cu-Fe sulfide, villamaninite (Cu, Ni, Co, Fe) S_2, and an unidentified Co-S phase with minor Cu and Fe along gypsum bedding planes by EDS and SEM.

https://doi.org/10.5194/egusphere-2023-607
Preprint. Discussion started: 12 April 2023

Previous research suggests that possible sources of mineralization of the Boleo deposits include hydrothermal leaching of underlying volcanic sequences and crystalline basement surrounding rocks (Ochoa-Landín, 1998), leaching of conglomerates by hydrothermal or meteoric fluids (Conly et al., 2001), and mineral-rich magmatic water separated from magmas solutions coeval with Boleo sedimentation (Conly, 2003; Conly et al., 2001). However, there has been no consideration of the role of the evaporite on the mineralization, even though evaporites have been recognized to have an active or passive role on supplying halogens to ore-making hydrothermal fluids (Pirajno, 2018). Cobalt sulfide minerals in the Boleo ore might have been deposited due to bacterially reduced sulfur carried in sulfate bearing-fluids, thus creating a suitable setting for the precipitation of metal sulfides when these solutions intermingled with metalliferous brine fluids (Warren, 2000). Previous studies seem to support the exchange of these two types of fluids based on the negative sulfur isotopes values (δ^{34} S < -15 ‰) for the pyrite-rich manto units reported by Ochoa-Landín (1998) and the less negative (δ^{34}S -8.0 to 1.8 ‰) high-temperature bacterial sulfate reduction (>80°C) of the sulfide mineralization stated by Conly (2003). Theoretical modeling of metal source, transport and deposition in sediment-hosted copper deposits has shown that cobalt sulfides precipitate within 50 cm of the sediment surface during bacterial sulfate reduction (Haynes and Bloom, 1987). Moreover, hydrothermal mobilization of cobalt can lead to ore grade concentration if the ore fluids are saline and oxidized. Cobalt can effectively be deposited as a sulfide mineral in lower temperatures in response to a sudden decline in fugacity (Vasyukova and Williams-Jones, 2022). Young high-K hornblende-bearing and high-Mg andesitic flows with ages of 7.73 +- 0.22 and 6.06 +- 0.27 Ma, respectively, have been proposed as a possible magmatic and heat source for the hydrothermal system of the Boleo deposit (Conly et al., 2005; Busby et al., 2020). However, it is not unreasonable to think that rift-transitional basalt and basaltic andesites rocks of Cerro Juanita (9.66 +- 0.21 Ma) and Cerro Sombrero Montado (8.84 +- 0.16 Ma) (Busby et al., 2020), may have also provided additional heat source since deprivation of mantle lithosphere by rifting or the opening of a slab window can last millions of years (Busby et al., 2020). Furthermore, a rift setting can induce migration of hydrothermal brine fluids by compaction upward and outward from rifts, causing leaching of mafic rocks with a high degree of partial melting and cobalt enrichment due to fractional crystallization (Ochoa-Landín, 1998; Vasyukova and Williams-Jones, 2022). In addition, saline water composition can control the maximum concentrations of copper-cobalt with sediments derived from basalt provenance (Haynes and Bloom, 1987). For example, freshly deposited unweathered, volcanic clasts of basalt and andesite-basaltic composition within the conglomerate facies of the Boleo Fm could have provided an additional metal source for brine fluids to transport, and if these brine fluids were heated, the higher mobility of cobalt compared to copper would have been able to travel farther before being precipitated by reduced sulfur (Annels and Simmonds, 1984).

6. Conclusions

The relation of the proto-Gulf of California rifting with the mineralization of the Boleo ore deposit is particularly clear as the Boleo clastic sequence records the stacking of multiple prograding fan-delta cycles with from marine to fluvial marine-environment in an evaporitic basin, what is now the present Santa Rosalia Basin. The Santa Rosalia basin represents a first-

https://doi.org/10.5194/egusphere-2023-607
Preprint. Discussion started: 12 April 2023

order sub-basin with at least two, second-order sub-basins, known as the north and south sub-basins with cobalt mineralization potential. Distribution of cobalt mineralization from trace mineralogy of the gypsum beds, high cobalt values from drill hole data and XRF field data suggest an interface of localized metal-rich magmatic hydrothermal fluids mixing with highly saline fluids of surficial or connate source. In the Boleo deposit, highly saline fluids circulated by convection through the mafic-rich minerals of the calc-alkaline volcanic rocks or rift-transition mafic rocks, enhancing cobalt mineralization capability in these fluids. Tectonism and changes in pressure in a rift transition setting, induce pumping rich mineralized fluids to an evaporitic basin. Additionally, as these fluids were making it to the surface, the presence of unweathered basaltic conglomerates of the Boleo Formation created small and local enrichment within the Boleo conglomerate when leached by these fluids. Finally, the distribution and presence of cobalt mineralization indicates that cobalt-rich fluids were transported along with sulfate fluids, and cobalt sulfide deposition occurred proximal to the sulfate reduction fronts of a highly saline reduced brines with organic-rich and sulfide-bearing environment.

Data availability

All shapefiles produced from Leapfrog and QGIS are available on request from the corresponding author.

Supplement

The supplement related to this article is available online at:

Author contributions

VOSM conceptualised the study and developed the methodology. AT, ATM, and AJJG helped in the field work data collection, petrographic analysis, and thin sections. JBM performed the laboratory work on the SEM and XRD analysis. VOSM drafted the original version with help of TMN and TMN helped with the final edition.

Competing interests

I Valente Octavio Salgado Muñoz declare that I have no known competing financial interests or personal relationships that could have appeared to influence the work reported in this paper.

Disclaimer

Publisher's note: Copernicus Publications remains neutral with regard to jurisdictional claims in published maps and institutional affiliations.

Acknowledgements

This study was supported in part by National Science Foundation grants EAR-1358347 and OISE-1826978 to Niemi and a research grant from the University of Missouri-Kansas City School of Graduate Studies and Earth and Environmental Sciences Department Newcomb grant to Salgado Muñoz. We thank Minera Boleo mine for access and logistical support for this project.

Financial support

https://doi.org/10.5194/egusphere-2023-607
Preprint. Discussion started: 12 April 2023

This research has been supported by National Science Foundation grants EAR-1358347 and OISE-1826978 to Niemi and a research grant from the University of Missouri-Kansas City School of Graduate Studies and Earth and Environmental Sciences Department Newcomb grant to Salgado Muñoz.

References

Angelier, J., Colletta, B., Chorowicz, J., Ortlieb, L., and Rangin, C.: Fault tectonics of the Baja California Peninsula and the opening of the Sea of Cortez, Mexico, Journal of Structural Geology, 3, 347–357, https://doi.org/10.1016/0191-8141(81)90035-3, 1981.

Annels, A. E. and Simmonds, J. R.: Cobalt in the Zambian Copperbelt, Precambrian Research, 25, 75–98, https://doi.org/10.1016/0301-9268(84)90025-1, 1984.

Bailes, R. J., Christoffersen, J. E., Escandon V., F., and Peatfield, G. R.: Sediment-Hosted Deposits of the Boléo Copper-Cobalt-Zinc District, Baja California Sur, Mexico, in: New Mines and Discoveries in Mexico and Central America, vol. 8, edited by: Albinson, T. and Nelson, C. E., Society of Economic Geologists, 0, https://doi.org/10.5382/SP.08.18, 2001.

Brown, A. C.: Sediment-hosted Stratiform Copper Deposits, Geol Canada, 19(3), 1992.

Busby, C., Graettinger, A., Martínez, M. L., Medynski, S., Niemi, T., Andrews, C., Bowman, E., Gutierrez, E. P., Henry, M., Lodes, E., Ojeda, J., Rice, J., Andrews, G., and Brown, S.: Volcanic record of the arc-to-rift transition onshore of the Guaymas basin in the Santa Rosalía area, Gulf of California, Baja California, Geosphere, 16, 1012–1041, https://doi.org/10.1130/GES02094.1, 2020.

Calmus, T., Aguillón-Robles, A., Maury, R. C., Bellon, H., Benoit, M., Cotten, J., Bourgois, J., and Michaud, F.: Spatial and temporal evolution of basalts and magnesian andesites ("bajaites") from Baja California, Mexico: the role of slab melts, Lithos, 66, 77–105, https://doi.org/10.1016/S0024-4937(02)00214-1, 2003.

Carreño, A. L.: Ostracodos y foraminiferos planctonicos de la Loma del Tirabuzon, Santa Rosalia, Baja California Sur, e implicaciones bioestratigraficas y paleoecologicas, Revista Mexicana de Ciencias Geológicas, 5, 55–64, 1981.

Conly, A. G.: Origin of the Boléo Cu-Co-Zn deposit, Baja California Sur, México: Implications for the interaction of magmatic-hydrothermal fluids in a low-temperature hydrothermal system, 2003.

Conly, A. G., Scott, S. D., Bellon, H., and Beaudoin, G.: The Boléo Cu-Co-Zn deposit, Baja California Sur, Mexico: the role of magmatic fluids in the genesis of a synsedimentary deposit, in: Mineral Deposits at the Beginning of the 21st Century, CRC Press, 223–226, 2001.

Conly, A. G., Brenan, J. M., Bellon, H., and Scott, S. D.: Arc to rift transitional volcanism in the Santa Rosalia region, Baja California Sur, Mexico, Journal of Volcanology and Geothermal Research, 142, 303–341, https://doi.org/10.1016/j.jvolgeores.2004.11.013, 2005.

Conly, A. G., Beaudoin, G., and Scott, S. D.: Isotopic constraints on fluid evolution and precipitation mechanisms for the Boléo Cu–Co–Zn district, Mexico, Mineralium Deposita, 41, 127–151, https://doi.org/10.1007/s00126-005-0045-3, 2006.

Conly, A. G., Scott, S. D., and Bellon, H.: Metalliferous manganese oxide mineralization associated with the Boléo Cu-Co-Zn district, Mexico, Economic Geology, 106, 1173–1196, 2011.

https://doi.org/10.5194/egusphere-2023-607
Preprint. Discussion started: 12 April 2023

Del Rio Salas, R., Ruiz, J., Ochoa-Landín, L., Noriega, O., Barra, F., Meza-Figueroa, D., and Paz-Moreno, F.: Geology, Geochemistry and Re–Os systematics of manganese deposits from the Santa Rosalía Basin and adjacent areas in Baja California Sur, México, Miner Deposita, 43, 467–482, https://doi.org/10.1007/s00126-008-0177-3, 2008.

Del Rio-Salas, R.: Metallogenesis for the Boléo and Cananea Copper Mining District: a contribution to the understanding of copper ore deposits in Northwestern Mexico., Ph.D. thesis, University of Arizona, Tucson U.S.A., 259 pp., 2011.

Del Rio-Salas, R., Ochoa-Landín, L., Eastoe, C. J., Ruiz, J., Meza-Figueroa, D., Valencia-Moreno, M., Zúñiga-Hernández, H., Zúñiga-Hernández, L., Moreno-Rodríguez, V., and Mendívil-Quijada, H.: Genesis of manganese oxide mineralization in the Boleo region and Concepción Peninsula, Baja California Sur: constraints from Pb-Sr isotopes and REE geochemistry, Revista mexicana de ciencias geológicas, 30, 482–499, 2013.

Dorsey, R. J., Niemi, T., Darin, M. H., Salgado Munoz, V., Bennett, S. E. K., Pecha, M., Usher, E., Elconin, L., Gardner, K., Brelle, B., Lira-Mijares, M., McCann, K., Jaime-Geraldo, A., Maher, A., and Henry, M.: Stratigraphy, sedimentology, age, and tectonic significance of the upper Miocene Boleo Formation in the Santa Rosalia Basin Baja California Sur, Mexico, GSA, https://doi.org/10.1130/abs/2022AM-381103, 2022.

Fletcher, J. M., Grove, M., Kimbrough, D., Lovera, O., and Gehrels, G. E.: Ridge-trench interactions and the Neogene tectonic evolution of the Magdalena shelf and southern Gulf of California: Insights from detrital zircon U-Pb ages from the Magdalena fan and adjacent areas, GSA Bulletin, 119, 1313–1336, https://doi.org/10.1130/B26067.1, 2007.

Gawthorpe, R. L. and Leeder, M. R.: Tectono-sedimentary evolution of active extensional basins, Basin Research, 12, 195–218, https://doi.org/10.1111/j.1365-2117.2000.00121.x, 2000.

Graettinger, A., Busby, C., McEnaney, T., Mindrup, Q., and Niemi, T.: Volcanology and structure of the Mulegé -Bahia Concepción Region, Gulf of California, Baja California Sur, Mexico: results from the Baja Basin Research Experience for Undergraduates (REU) and International Research Experience for Students (IRES), GSA, https://doi.org/10.1130/abs/2022AM-382213, 2022.

Hardie, L. A., Lowenstein, T., and Spencer, R.: The problem of distinguishing between primary and secondary features in evaporites, Sixth International Symposium on Salt, 1, 11–39, 1985.

Hausback, B.: Cenozoic volcanic and tectonic evolution of Baja California, Mexico, Geology of the Baja California Peninsula, 219–236, 1984.

Haynes, D. W. and Bloom, M. S.: Stratiform copper deposits hosted by low-energy sediments; III, Aspects of metal transport, Economic Geology, 82, 635–648, https://doi.org/10.2113/gsecongeo.82.3.635, 1987.

Hitzman, M., Bookstrom, A., Slack, J., and Zientek, M.: Cobalt-Styles of Deposits and the Search for Primary Deposits; US Department of the Interior, US Geological Survey: Denver, CO, USA, 47, https://doi.org/10.3133/ofr20171155, 2017.

Hitzman, M. W., Selley, D., and Bull, S.: Formation of sedimentary rock-hosted stratiform copper deposits through Earth history, Economic Geology, 105, 627–639, https://doi.org/10.2113/gsecongeo.105.3.627, 2010.

Holt, J. W., Holt, E. W., and Stock, J. M.: An age constraint on Gulf of California rifting from the Santa Rosalía basin, Baja California Sur, Mexico, GSA Bulletin, 112, 540–549, https://doi.org/10.1130/0016-7606(2000)112<540:AACOGO>2.0.CO;2, 2000.

Kendall, A.: Marine Evaporites, in: Facies Model 4, Geological Association of Canada, 586 pp505–539, 2010.

https://doi.org/10.5194/egusphere-2023-607
Preprint. Discussion started: 12 April 2023

Kirkham, R. V.: Distribution, settings, and genesis of sediment-hosted stratiform copper deposits, Geological Association of Canada Special Paper, 36, 3–38, 1989.

Lonsdale, P.: Geology and tectonic history of the Gulf of California, in: The Eastern Pacific Ocean and Hawaii, vol. N, edited by: Winterer, E. L., Hussong, D. M., and Decker, R. W., Geological Society of America, 0, https://doi.org/10.1130/DNAG-GNA-N.499, 1989.

Matano, F.: The 'Evaporiti di Monte Castello' deposits of the Messinian Southern Apennines foreland basin (Irpinia–Daunia Mountains, Southern Italy): stratigraphic evolution and geological context, in: Evaporites Through Space and Time, vol. 285, edited by: Schreiber, B. C., Lugli, S., and Bąbel, M., Geological Society of London, 0, https://doi.org/10.1144/SP285.12, 2007.

Miller, N. C. and Lizarralde, D.: Thick evaporites and early rifting in the Guaymas Basin, Gulf of California, Geology, 41, 283–286, https://doi.org/10.1130/G33747.1, 2013.

Miranda-Martínez, A. Y., Carreño, A. L., and McDougall, K.: The Neogene genus Streptochilus (Brönnimann and Resig, 1971) from the Gulf of California, Marine Micropaleontology, 132, 35–52, https://doi.org/10.1016/j.marmicro.2017.05.001, 2017.

Muchez, Ph. and Corbella, M.: Factors controlling the precipitation of copper and cobalt minerals in sediment-hosted ore deposits: Advances and restrictions, Journal of Geochemical Exploration, 118, 38–46, https://doi.org/10.1016/j.gexplo.2012.04.006, 2012.

Müller, D. W., Mueller, P., and McKenzie, J.: Strontium Isotopic Ratios as Fluid Tracers in Messinian Evaporites of the Tyrrhenian Sea (Western Mediterranean Sea), in: Proc. ODP Sci. Results, vol. 107, 603–614, https://doi.org/10.2973/odp.proc.sr.107.194.1990, 1990.

Niemi, T., Graettinger, A., Salgado Munoz, V., Murowchick, J., Busby, C., Martinez Gutierrez, G., Antinao Rojas, J. L., Dorsey, R. J., Darin, M. H., and Gardner, K.: The Baja Basins Program: mentored undergraduate field and lab research integrating multidisciplinary geologic data to address the tectonic evolution of the Gulf of California rift of the east-central Baja Peninsula, México., GSA, https://doi.org/10.1130/abs/2022AM-380608, 2022.

Ochoa-Landín, L., Ruiz, J., Calmus, T., Perez Segura, E., and Escandon, F.: Sedimentology and Stratigraphy of the Upper Miocene El Boleo Formation, Santa Rosalía, Baja California, México., Revista Mexicana de Ciencias Geológicas, 17, 83–96, 2000.

Ochoa-Landín, L. H.: Geological, sedimentological and geochemical studies of the Boleo copper-cobalt-zinc deposit, Santa Rosalia, Baja California, Mexico, Ph.D. thesis, University of Arizona, Tucson U.S.A., 148 pp., 1998.

Ortlieb, L. and Colleta, B.: Sintesis cronoestratigrafica sobre el Neogeno y el Cuaternario marino de la cuenca de Santa Rosalia, Baja California Sur, Mexico- fdi:15453- Horizon, 1984.

Pirajno, F.: Halogens in Hydrothermal Fluids and Their Role in the Formation and Evolution of Hydrothermal Mineral Systems, in: The Role of Halogens in Terrestrial and Extraterrestrial Geochemical Processes: Surface, Crust, and Mantle, edited by: Harlov, D. E. and Aranovich, L., Springer International Publishing, Cham, 759–804, https://doi.org/10.1007/978-3-319-61667-4_12, 2018.

Salgado Muñoz, V.: Estratigrafía del manto 1 en la subcuenca Montado del proyecto Boleo, Santa Rosalía, Baja California Sur., Bachelor Thesis, Universidad Autonoma de Baja California Sur, Mexico, 83 pp., 2014.

https://doi.org/10.5194/egusphere-2023-607
Preprint. Discussion started: 12 April 2023

Salgado Muñoz, V., Niemi, T., Murowchick, J., and Penaflor, G.: Sedimentary and geochemical analysis of the gypsum unit in the Boleo Copper Deposit, Santa Rosalia Basin, Mexico., Society of Economic Geologist, Keystone Colorado U.S.A/, 2018.

Schreiber, B. C., Friedman, G. M., Decima, A., and Schreiber, E.: Depositional environments of Upper Miocene (Messinian) evaporite deposits of the Sicilian Basin, Sedimentology, 23, 729–760, https://doi.org/10.1111/j.1365-3091.1976.tb00107.x, 1976.

Schreiber, B. C., Lugli, S., and Babel, M.: Evaporites through space and time, Geological Society ; Distributors, North America, for individual and Corporate orders, AAPG Bookstore, London, Tulsa, OK, 373 pp., 2007.

Selley, D., Scott, R., Emsbo, P., Koziy, L., Hitzman, M. W., Bull, S. W., Duffett, M., Sebagenzi, S., Halpin, J., and Broughton, D. W.: Structural Configuration of the Central African Copperbelt: Roles of Evaporites in Structural Evolution, Basin Hydrology, and Ore Location, in: Metals, Minerals, and Society, vol. 21, edited by: Arribas R., A. M. and Mauk, J. L., Society of Economic Geologists (SEG), 0, https://doi.org/10.5382/SP.21.07, 2018.

Smith, C. G.: Always the bridesmaid, never the bride: cobalt geology and resources, Applied Earth Science, 110, 75–80, https://doi.org/10.1179/aes.2001.110.2.75, 2001.

Stock, J. M. and Hodges, K. V.: Pre-Pliocene Extension around the Gulf of California and the transfer of Baja California to the Pacific Plate, Tectonics, 8, 99–115, https://doi.org/10.1029/TC008i001p00099, 1989.

Sutherland, F. H., Kent, G. M., Harding, A. J., Umhoefer, P. J., Driscoll, N. W., Lizarralde, D., Fletcher, J. M., Axen, G. J., Holbrook, W. S., González-Fernández, A., and Lonsdale, P.: Middle Miocene to early Pliocene oblique extension in the southern Gulf of California, Geosphere, 8, 752–770, https://doi.org/10.1130/GES00770.1, 2012.

Umhoefer, P. J., Darin, M. H., Bennett, S. E. K., Skinner, L. A., Dorsey, R. J., and Oskin, M. E.: Breaching of strike-slip faults and successive flooding of pull-apart basins to form the Gulf of California seaway from ca. 8–6 Ma, Geology, 46, 695–698, https://doi.org/10.1130/G40242.1, 2018.

Vasyukova, O. V. and Williams-Jones, A. E.: Constraints on the Genesis of Cobalt Deposits: Part II. Applications to Natural Systems, Economic Geology, 117, 529–544, https://doi.org/10.5382/econgeo.4888, 2022.

Wang, Y., Forsyth, D. W., Rau, C. J., Carriero, N., Schmandt, B., Gaherty, J. B., and Savage, B.: Fossil slabs attached to unsubducted fragments of the Farallon plate, Proceedings of the National Academy of Sciences, 110, 5342–5346, https://doi.org/10.1073/pnas.1214880110, 2013.

Warren, J. K.: Evaporites, brines and base metals: Low-temperature ore emplacement controlled by evaporite diagenesis, Australian Journal of Earth Sciences, 47, 179–208, https://doi.org/10.1046/j.1440-0952.2000.00781.x, 2000.

Warren, J. K.: Evaporites: A Geological Compendium, Springer International Publishing, Cham, https://doi.org/10.1007/978-3-319-13512-0, 2016.

Wilson, I. and Rocha, V.: Geology and mineral deposits of the Boleo copper district, Baja California, Mexico., US Government Printing Office, 134 pp., 1955.

Wilson, I. and Veytia, M.: Geology and Manganese Deposits of the Lucifer District Northwest of Santa Rosalia Baja California, Mexico, US Government Printing Office, 177–233 pp., 1949.